



UNIVERSITÀ POLITECNICA DELLE MARCHE
Repository ISTITUZIONALE

Enhanced trajectory tracking using optimally combined feedforward plant inversion and feedforward closed loop inversion

This is the peer reviewed version of the following article:

Original

Enhanced trajectory tracking using optimally combined feedforward plant inversion and feedforward closed loop inversion / Jetto, Leopoldo; Orsini, Valentina. - In: EUROPEAN JOURNAL OF CONTROL. - ISSN 0947-3580. - 63:(2022), pp. 223-231. [10.1016/j.ejcon.2021.11.004]

Availability:

This version is available at: 11566/294535 since: 2024-05-07T09:59:58Z

Publisher:

Published

DOI:10.1016/j.ejcon.2021.11.004

Terms of use:

The terms and conditions for the reuse of this version of the manuscript are specified in the publishing policy. The use of copyrighted works requires the consent of the rights' holder (author or publisher). Works made available under a Creative Commons license or a Publisher's custom-made license can be used according to the terms and conditions contained therein. See editor's website for further information and terms and conditions.

This item was downloaded from IRIS Università Politecnica delle Marche (<https://iris.univpm.it>). When citing, please refer to the published version.

(Article begins on next page)

Enhanced trajectory tracking using optimally combined feedforward plant inversion and feedforward closed loop inversion

Leopoldo Jetto, Valentina Orsini

Dipartimento di Ingegneria dell'Informazione, Università Politecnica delle Marche, Ancona, Italy, (L.Jetto@univpm.it, vorsini@univpm.it).

Abstract

This paper focuses on the problem of determining the most appropriate Two Degrees of Freedom (2DoF) control architecture, when the FeedForward (FF) action is the result of a stable model inversion procedure. The purpose is to define a control scheme with enhanced tracking performance even in the case of non minimum phase MIMO plant affected by polytopic uncertainty and with a possible non hyperbolic internal dynamics. The new proposed 2DoF architecture is given by an optimal balance of the control actions produced by FeedForward Plant Inversion (FFPI) and FeedForward Closed Loop Inversion (FFCLI). This new architecture is referred to as FeedForward Optimally Balanced Inversion (FFOBI). Robustness with respect to polytopic uncertainty is obtained using a min-max optimization approach. Numerical results show that the FFOBI improves the tracking of both FFPI and FFCLI.

Keywords: Output tracking, 2DoF control, model inversion, parametric uncertainty.

1. Introduction

The well established theoretical framework of model inversion [1]-[11] provides a powerful tool to define 2DoF control schemes based on a FeedForward (FF) inverting control action. This allows overcoming many limitations of classical 1DoF control schemes.

For practical applications to output tracking problems, the most widely used 2DoF control architectures based on inverse control can be classified into two main categories: FeedForward Plant Inversion (FFPI) (see e.g. [12] -[18]), and FeedForward Closed Loop Inversion (FFCLI) (see e.g. [19]-[22]). In the FFPI methods the FF control is obtained through a plant model inversion procedure, in the FFCLI the FF input is obtained inverting the closed-loop system. With reference to some SISO plants, the performances of the two architectures are discussed and compared in [23]-[27]. These papers evidence that the achievable

tracking accuracy of both control schemes depend on the specific application and on the amount of uncertainty affecting the plant. As each of the two architectures has advantages over the other, it would be very useful to define a more general 2DoF control architecture optimally combining the FFPI and FFCLI control actions independently of the particular application. This problem can not be solved with the guidelines stated in the above papers because they refer to some specific applications and their qualitative nature makes it difficult any generalization.

In the case of exact model inversion of linear continuous-time SISO plants, the equivalence of FFPI and FFCLI control schemes has been recently proved in [28]. However, exact model inversion methods require an infinite pre-actuation interval, therefore, in practical applications they are replaced by approximate inversion methods (see e.g. the above cited references [13]–[27] and references therein).

The problem considered in this paper is precisely to define a systematic approximate inversion method for MIMO plants to obtain an FF control law such that: i) it is always given by an optimal combination of the FFPI and FFCLI control actions independently of the particular application, ii) it is robust with respect to polytopic uncertainties affecting the MIMO plant to be controlled. To the best of the authors' knowledge this is still an open problem.

The proposed approach is based on some theoretical results concerning the notion of pseudo-inversion and B-splines input parametrization [6], [29]–[32]. The results of these references are here extended to deal with a robust, generalized inversion problem involving the simultaneous pseudo-inversion of two different polytopic control schemes. A further relevant novelty of the present contribution is a more convenient formulation of the optimization problem leading to a numerically simplified on-line solution procedure. A short simplified version of this contribution has been presented in [33].

The design of the FFOBI architecture proposed in this paper can be summarized in the two following steps.

Step 1). Given an LTI, continuous-time, polytopic plant Σ_p , an LTI dynamic output feedback controller is designed to guarantee the robust stability of the closed-loop system Σ_f . The controller is also endowed with an internal model of the steady-state component of the desired output $y_d(t)$ to be tracked.

Step 2). Σ_f is forced by two inputs $r_1(t)$ and $r_2(t)$ affinely depending on the outputs $\mathbf{s}_1(t)$ and $\mathbf{s}_2(t)$ of two feedforward input estimators IE_1 and IE_2 simultaneously operating according to the FFCLI and FFPI schemes respectively. The two signals $\mathbf{s}_1(t)$ and $\mathbf{s}_2(t)$ are searched in the linear space generated by B-spline basis functions of a fixed degree and are computed so that the corresponding $r_1(t)$ and $r_2(t)$ solve a "worst-case" optimization problem.

Remark 1. It is here stressed that the purpose of the paper is not designing the FB controller (Step 1). Rather, the paper is focused on the design of the optimal FF control action (Step 2). \triangle

Parametrizing $\mathbf{s}_1(t)$ and $\mathbf{s}_2(t)$ as B-splines involves significant advantages: B-spline functions are continuously differentiable universal approximators which admit a parsimonious parametric representation and belong to the convex hull

defined by the relative control points [34]. These properties significantly reduce the number of parameters (the control points) with respect to the quadratic cost functional is minimized. They also allow the minimization procedure to be formulated as a robust least square estimation problem where both the design matrix and observations are not exactly known due to plant uncertainty. The resulting optimal feedforward action is given by the optimal balance of the two contributions produced by FFPI and FFCLI control scheme because the estimated control points univocally define the corresponding B-splines and hence the corresponding $r_1(t)$ and $r_2(t)$. The weights of the two contributions are given by the 2-norms of the estimated B-splines. During the transient period, the optimal inputs are applied to Σ_f according to a Receding Horizon Control (RHC) to improve robustness with respect to parametric uncertainties.

The paper is organized in the following way. Some mathematical preliminaries are recalled in Section 2. The FFOBI control architecture and problem statement are given in Section 3. The problem solution is reported in Sections 4 and 5. The numerical example of Section 6 shows the application of the proposed method to a robust trajectory tracking problem for the same Bell 205 Helicopter considered in [35].

2. Mathematical Background

2.1. B-spline functions [34]

A scalar B-spline time function is defined as a linear combination of B-splines basis functions and control points:

$$s(t) = \sum_{i=1}^{\ell} c_i B_{i,d}(t), \quad t \in [\hat{t}_1, \hat{t}_{\ell+d+1}] \subseteq \mathbb{R}, \quad (1)$$

where the c_i 's are real numbers representing the control points of $s(t)$, the integer d is the degree of the B-spline, the $(\hat{t}_i)_{i=1}^{\ell+d+1}$ are the non decreasing knot points and the $B_{i,d}(t)$ are the B-spline basis functions which can be computed by the Cox-de Boor recursion formula, [34]. An equivalent representation of $s(t)$ in (1) is

$$s(t) = \mathbf{B}_d(t) \mathbf{c}, \quad t \in [\hat{t}_1, \hat{t}_{\ell+d+1}] \subseteq \mathbb{R}, \quad (2)$$

where $\mathbf{c} \triangleq [c_1, \dots, c_{\ell}]^T$ and $\mathbf{B}_d(t) \triangleq [B_{1,d}(t), \dots, B_{\ell,d}(t)]$.

Convex hull property. Any value assumed by $s(t)$, $\forall t \in [\hat{t}_j, \hat{t}_{j+1}]$, $j > d$, lies in the convex hull of its $d+1$ control points c_{j-d}, \dots, c_j . \triangle

For a q -component vector $\mathbf{s}(t) = [s_1(t), \dots, s_q(t)]^T$, a compact B-spline representation can be used

$$\mathbf{s}(t) = \bar{\mathbf{B}}_d(t) \bar{\mathbf{c}}, \quad t \in [\hat{t}_1, \hat{t}_{\ell+d+1}], \quad (3)$$

where $\bar{\mathbf{c}} \triangleq [\mathbf{c}_1^T, \dots, \mathbf{c}_q^T]^T$ and $\bar{\mathbf{B}}_d(t) \triangleq \text{diag}[\mathbf{B}_d(t), \dots, \mathbf{B}_d(t)]$. Each $\mathbf{c}_i \triangleq [c_{i,1}, \dots, c_{i,\ell}]^T$, $i = 1, \dots, q$, is defined as in (2). The dimensions of $\bar{\mathbf{c}}$ are $(q\ell \times 1)$. The dimensions of the block diagonal matrix $\bar{\mathbf{B}}_d(t)$ are $(q \times q\ell)$.

Remark 2. From (2) it is apparent that, once the degree d and the knot points \hat{t}_i have been fixed, the scalar B spline function $s(t)$, $t \in [\hat{t}_1, \hat{t}_{\ell+d+1}]$, is completely determined by the corresponding vector \mathbf{c} of ℓ control points. \triangle

2.2. The robust least squares problem [36]

Given an overdetermined set of linear equations $Df \approx g$, with $D \in \mathbb{R}^{r \times m}$, $g \in \mathbb{R}^r$, subject to unknown but bounded errors: $\|\delta D\|_s \leq \rho$ and $\|\delta g\|_s \leq \xi$, the robust least squares estimate $\hat{f} \in \mathbb{R}^m$ is the value of f minimizing

$$\min_f \max_{\|\delta D\|_s \leq \rho, \|\delta g\|_s \leq \xi} \|(D + \delta D)f - (g + \delta g)\|, \quad (4)$$

where $\|\cdot\|_s$ denotes the spectral norm.

As shown in ([36], p. 206), problem (4) is equivalent to minimizing a sum of Euclidean norms

$$\min_f \|Df - g\| + \rho\|f\| + \xi \quad (5)$$

Possible constraints on f of the kind

$$\underline{f} \leq f \leq \bar{f} \quad (6)$$

can be taken into account by imposing all the scalar linear inequalities deriving from the above vector constraint.

3. The FFOBI control scheme and problem statement

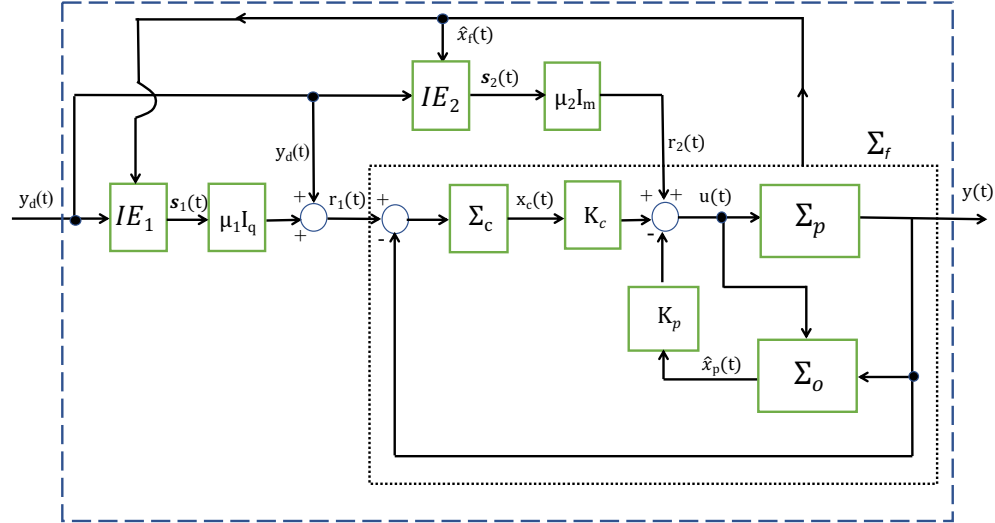


Figure 1: The FFOBI control scheme

The new 2DoF control scheme proposed in this paper is shown in Fig. 1 where, without any loss of generality, a unitary feedback is assumed. The two blocks IE_1 and IE_2 are two feedforward input estimators operating according to the FFCLI and FFPI schemes respectively. The inputs of both feedforward filters are the desired output $y_d(t)$ to be tracked and the estimated state $\hat{x}_f(t)$ of Σ_f . The outputs of IE_1 and IE_2 are the two B-splines $\mathbf{s}_1(t) \in \mathbb{R}^q$ and $\mathbf{s}_2(t) \in \mathbb{R}^m$ respectively. The two scalars μ_1 and μ_2 are two binary variables. The FFOBI control scheme optimally combining the FFCLI and FFPI architectures corresponds to $\mu_1 = \mu_2 = 1$. If $\mu_1 = 1$ and $\mu_2 = 0$, then $r_1(t) = y_d(t) + \mathbf{s}_1(t)$ and $r_2(t) = 0$, so that the FFCLI is obtained, while $\mu_1 = 0$ and $\mu_2 = 1$ give $r_1(t) = y_d(t)$ and $r_2(t) = \mathbf{s}_2(t)$, so that the FFPI is obtained. For $\mu_1 = \mu_2 = 0$, the 2DoF control scheme reduces to the usual 1DoF feedback control scheme with no feedforward action.

The block Σ_f is the feedback connection of a (possibly non-minimum phase and/or with non hyperbolic internal dynamics) LTI polytopic plant Σ_p with an LTI robustly stabilizing dynamic output feedback controller. The plant $\Sigma_p \equiv (C_p, A_p(\alpha), B_p)$ is given by

$$\dot{x}_p(t) = A_p(\alpha)x_p(t) + B_p u(t), u(t) \in \mathbb{R}^m, \quad (7)$$

$$y(t) = C_p x_p(t), y(t) \in \mathbb{R}^q, \quad (8)$$

where: $x_p(t) \in \mathbb{R}^{n_p}$, $A_p(\alpha) \in \mathcal{A} \triangleq \text{co}\{A_{p_i}, \dots, A_{p_l}\} = \{A_p(\alpha) = \sum_{i=1}^l \alpha_i A_{p_i}\}$, and the vector $\alpha = [\alpha_1, \dots, \alpha_l]^T$ belongs to the unit simplex Λ_l defined as $\Lambda_l = \{\alpha : \sum_{i=1}^l \alpha_i = 1, \alpha_i \geq 0\}$.

The following assumptions on Σ_p are made:

- A1):** Σ_p is robustly stabilizable by an LTI dynamic output controller;
- A2)** let the steady state component $\tilde{y}_d(t)$ of the desired output trajectory $y_d(t)$ be generated as the free output response of an LTI unstable system Σ_y , then for no $\alpha \in \Lambda_l$, Σ_p has a transmission zero coinciding with an eigenvalue of the dynamical matrix of Σ_y .

The dynamic output feedback controller includes the internal model Σ_c of the steady state component of the desired output trajectory $y_d(t)$, whose state-space has the form $\dot{x}_c(t) = A_c x_c(t) + B_c(r_1(t) - y(t))$ ($x_c(t) \in \mathbb{R}^{n_c}$) for suitably defined A_c and B_c [37], and a full state observer Σ_o of the form

$$\dot{\hat{x}}_p(t) = \bar{A}_p \hat{x}_p(t) + B_p u(t) + L(y(t) - C_p \hat{x}_p(t)), \quad (9)$$

where: $\bar{A}_p \triangleq (\sum_{i=1}^l A_{p_i})/l$ is the assumed nominal dynamical matrix of the plant.

The input $u(t) \in \mathbb{R}^m$ forcing the polytopic plant Σ_p is given by

$$u(t) = -K_p \hat{x}_p(t) + K_c x_c(t) + r_2(t). \quad (10)$$

The state space $(C_f, A_f(\alpha), B_f)$ of the closed loop system Σ_f with $x_f(t) \triangleq [x_p^T(t), x_c^T(t), \hat{x}_p^T(t)]^T \in \mathbb{R}^n$, $n \triangleq 2n_p + n_c$ and $r(t) \triangleq [r_1^T(t), r_2^T(t)]^T \in \mathbb{R}^{q+m}$

is

$$\begin{aligned}\dot{x}_f(t) &= \begin{bmatrix} A_p(\alpha) & B_p K_c & -B_p K_p \\ -B_c C_p & A_c & 0 \\ LC_p & B_p K_c & \bar{A}_p - LC_p - B_p K_p \end{bmatrix} x_f(t) \\ &+ \begin{bmatrix} 0 & B_p \\ B_c & 0 \\ 0 & B_p \end{bmatrix} r(t)\end{aligned}\quad (11)$$

$$y(t) = [C_p \ 0 \ 0] x_f(t) \quad (12)$$

where, analogously to $A_p(\alpha)$, also $A_f(\alpha) \in \mathcal{A}_f \triangleq \text{co}\{A_{f_i}, \dots, A_{f_l}\}$. By the way $x_f(t)$ and $r(t)$ are defined, $u(t)$ can be rewritten as

$$u(t) = [0 \ K_c \ -K_p] x_f(t) + [0 \ I] r(t). \quad (13)$$

The existence of matrices K_c , K and L such that Σ_f is internally asymptotically stable $\forall A_f(\alpha) \in \mathcal{A}_f$, is guaranteed by assumption **A1**. These matrices can be computed by any existing robust stabilizing technique. This problem is not discussed here because the focus of the paper is on computing an optimally balanced feedforward control action $r(t)$. The presence of the internal model Σ_c and **A2** guarantees robust exact asymptotic tracking even with no feedforward action [37]. Hence, the problem of determining an optimally combined feedforward action can be limited to a sufficiently long but finite interval over which steady-state is practically attained. This drastically reduces the computational burden of the numerical procedure for the minimization of the cost functional (see Section 5).

For this reason the following signals are partitioned in a transient and steady state component as follows:

$$y_d(t) = \begin{cases} y_{d,t}(t) & t \in [0, t_y) \triangleq T_y \\ \tilde{y}_d(t) & t \geq t_y \\ y_{d,t}(t_y^-) = \tilde{y}_d(t_y) \end{cases} \quad (14)$$

where $y_{d,t}(t)$ and $\tilde{y}_d(t)$ are smooth functions denoting the transient and steady state components of $y_d(t)$, respectively, T_y is the time interval over which $y_{d,t}(t)$ is required to converge towards $\tilde{y}_d(t)$.

Analogously:

$$\mathbf{s}_i(t) = \begin{cases} \mathbf{s}_{i,t}(t), & t \in [0, t_r) \triangleq T_r \\ \tilde{\mathbf{s}}_i(t), & t \geq t_r, \\ \mathbf{s}_{i,t}(t_r^-) = \tilde{\mathbf{s}}_i(t_r) \end{cases} \quad i = 1, 2 \quad (15)$$

$$r(t) = \begin{cases} r_t(t) \triangleq \begin{bmatrix} y_d(t) + \mu_1 \mathbf{s}_{1,t}(t) \\ \mu_2 \mathbf{s}_{2,t}(t) \end{bmatrix}, & t \in [0, t_r) \triangleq T_r \\ \tilde{r}(t) \triangleq \begin{bmatrix} \tilde{y}_d(t) + \mu_1 \tilde{\mathbf{s}}_1(t) \\ \mu_2 \tilde{\mathbf{s}}_2(t) \end{bmatrix}, & t \geq t_r \\ r_t(t_r^-) = \tilde{r}(t_r) \end{cases} \quad (16)$$

The time instant t_r has to be sufficiently large to guarantee that $r_t(t_r^-) = \tilde{r}(t_r)$ (namely $\mathbf{s}_{i,t}(t_r^-) = \tilde{\mathbf{s}}_i(t_r)$, $i = 1, 2$) and the actual output $y(t)$ under the action of $r_t(t)$ has almost achieved the steady-state trajectory. A way to fix a lower bound on t_r is: $t_r \geq t_s$, where t_s is the settling time relative to the output of the nominal $\bar{\Sigma}_f \triangleq (C_f, \bar{A}_f, B_f)$ forced by $r(t) = [y_d^T(t) \ 0^T]^T$. Like \bar{A}_p , also \bar{A}_f is chosen as the centroid of \mathcal{A}_f : $\bar{A}_f \triangleq \frac{\sum_{i=1}^l A_{fi}}{l}$.

Definition. The optimal combination of FFPI and FFCLI is the one giving a minimum 2-norm predicted transient tracking error.

By the above definition, the problem of optimally balancing FFPI and FFCLI can be restated as the following equivalent Robust Almost Exact Output Tracking Problem.

(RAEOTP) Let $\Sigma_f \equiv (C_f, A_f(\alpha), B_f)$ be a robustly asymptotically stable closed loop system described by (11), (12) with unknown initial state $x_f(0)$. Given a desired $y_d(t)$ defined as in (14), it is required to find a feedforward control input $r(t)$ defined as in (16) satisfying the following conditions $\forall A_f(\alpha) \in \mathcal{A}_f$:

Transient conditions: i) $r_t(t)$ is converging to $\tilde{r}(t_r)$ over T_r , ii) $r_t(t)$ is the result of an RHC strategy applied to the minimization of a suitably defined "worst case" quadratic cost functional of the predicted transient tracking error (see (17)-(19) of Section 4.2)

Steady-state condition: $\tilde{r}(t)$ yields a steady-state tracking error asymptotically converging to zero.

Boundedness condition: $r(t)$ is uniformly bounded for any uniformly bounded $y_d(t)$.

4. Computation of $r(t)$

In accordance with definition (16), this step is performed through a separate computation of the steady state $\tilde{r}(t)$ and transient $r_t(t)$ components of $r(t)$.

4.1. Computation of $\tilde{r}(t)$

As Σ_f is robustly asymptotically stable, then, by **A2**, the steady-state condition is automatically satisfied endowing the dynamic output feedback controller with the internal model of $\tilde{y}_d(t)$ [37]. Recalling the assumption of a unitary feedback, it is enough to choose $\tilde{s}_1(t) = \tilde{s}_2(t) = 0$, for $t \geq t_r$, which, by (16), implies $\tilde{r}(t) = [\tilde{y}_d^T(t) \ 0^T]^T$.

4.2. Computation of $r_t(t)$

In the following, the explicit dependence on α of the predicted output and tracking error will be omitted for simplicity of notation.

The robust optimization problem is numerically solved imposing to $r_{1,t}(t) = y_d(t) + \mu_1 \mathbf{s}_{1,t}(t)$ and $r_{2,t}(t) = \mu_2 \mathbf{s}_{2,t}(t)$ the structure deriving from the assumption of modeling the transient components of $\mathbf{s}_1(t)$ and $\mathbf{s}_2(t)$ respectively as B-spline functions given by (3). The parameter vector defining $r_t(t)$ is computed as the solution of the constrained optimization problem defined beneath.

Let $T'_r \triangleq [0, t_r + t_w)$ be partitioned as $T'_r = \bigcup_{k=0}^{n_r-1} T_k$, where $T_k \triangleq [t_k, t_k + t_w)$, $k = 0, 1, \dots, n_r - 1$, with $t_k \triangleq k\Delta$ and $\Delta \triangleq \frac{t_r}{n_r}$ are disjoint sub-intervals such that: $t_0 = 0, t_{n_r} = n_r\Delta = t_r$. According to the RHC strategy, $t_w = w\Delta$, denotes the length of the moving window T_k , for a fixed $w \in \mathbb{Z}^+$. The transient $r_t(t)$ is determined from the minimization of the following "worst case" quadratic cost functional for any fixed $k = 0, 1, \dots, n_r - 1$:

$$\max_{\alpha \in \Lambda_l} J_{k,\alpha} \triangleq \max_{\alpha \in \Lambda_l} \sum_{i=1}^{w-1} e^T(t_{k+i}|t_k) Q(t_k) e(t_{k+i}|t_k), \quad (17)$$

where

$$e(t_{k+i}|t_k) \triangleq y_d(t_{k+i}) - y(t_{k+i}|t_k), \quad (18)$$

with

$$\begin{aligned} y(t_{k+i}|t_k) &\triangleq C_f e^{A_f(\alpha)(t_{k+i}-t_k)} \hat{x}_f(t_k) \\ &+ \int_{t_k}^{t_{k+i}} C_f e^{A_f(\alpha)(t_{k+i}-\tau)} B_f r_t(\tau) d\tau, \end{aligned} \quad (19)$$

is the predicted tracking error at time t_{k+i} based on the state estimate $\hat{x}_f(t_k)$. By definition of $r_t(t)$ and according to (3) one has

$$\begin{aligned} r_t(t) &= \begin{bmatrix} \mu_1 \tilde{\mathbf{B}}_{d_1}(t) & 0 \\ 0 & \mu_2 \tilde{\mathbf{B}}_{d_2}(t) \end{bmatrix} \begin{bmatrix} \tilde{\mathbf{c}}_1 \\ \tilde{\mathbf{c}}_2 \end{bmatrix} + \begin{bmatrix} y_d(t) \\ 0 \end{bmatrix} \\ &\triangleq \tilde{\mathbf{B}}(t) \tilde{\mathbf{c}} + \mathbf{y}_d(t) \end{aligned} \quad (20)$$

where the integer d_1 (d_2) indicates the degree of the scalar B spline functions composing $r_{t,1}(t) \in \mathbb{R}^q$ ($r_{t,2}(t) \in \mathbb{R}^m$). The dimensions of $\tilde{\mathbf{c}}$ are $(q\ell_1 + m\ell_2) \times 1$. The dimensions of the block diagonal matrix $\tilde{\mathbf{B}}(t)$ are $(q + m) \times (q\ell_1 + m\ell_2)$. By (19),(20) and setting $\tilde{\mathbf{c}} = \tilde{\mathbf{c}}_k$, $e(t_{k+i}|t_k)$ results to be given by

$$\begin{aligned} e(t_{k+i}|t_k) &= y_d(t_{k+i}) - C_f e^{A_f(\alpha)(t_{k+i}-t_k)} \hat{x}_f(t_k) \\ &- \int_{t_k}^{t_{k+i}} C_f e^{A_f(\alpha)(t_{k+i}-\tau)} B_f \tilde{\mathbf{B}}(\tau) d\tau \tilde{\mathbf{c}}_k \\ &- \int_{t_k}^{t_{k+i}} C_f e^{A_f(\alpha)(t_{k+i}-\tau)} B_f \mathbf{y}_d(\tau) d\tau \end{aligned} \quad (21)$$

The input function $r_t(t), t \in T_r$, affinely dependent on $\mathbf{s}_{1,t}(t)$ and $\mathbf{s}_{2,t}(t)$, is robustly estimated minimizing the worst case error due to the parametric uncertainty. More precisely $r_t(t), t \in T_r$, is obtained solving the following sequence of n_r Min-Max Constrained Optimization Problems (MMCOP)

$$\text{MMCOP: } \min_{\tilde{\mathbf{c}}_k} \max_{\alpha \in \Lambda_l} J_{k,\alpha}, \quad k = 0, \dots, n_r - 1, \quad (22)$$

$$\text{subject to } \tilde{\mathbf{c}}_{k,\min} \leq \tilde{\mathbf{c}}_k \leq \tilde{\mathbf{c}}_{k,\max}. \quad (23)$$

At $k = 0$ ($t_0 = 0$), the MMCOP is solved with reference to a $J_{0,\alpha}$, which, by (17), is defined over $[t_0, t_0 + t_w) = [0, t_w)$ and the corresponding minimizing $\tilde{\mathbf{c}}_0$ defines $r_t(t)$ over the same interval. According to the RHC strategy only the restriction of $r_t(t)$ to $T_0 = [t_0, t_1)$ is applied to Σ_f . Analogously, for $k = 1$, ($t_1 = \Delta$), the minimizing $\tilde{\mathbf{c}}_1$ gives $r_t(t)$, $t \in [t_1, t_1 + t_w)$ but only $r_t(t)$, $t \in T_1 = [t_1, t_2)$ is applied. The iterative procedure stops at $k = n_r - 1$.

Over each moving window $[t_k, t_k + t_w)$, the constraints (23) on $\tilde{\mathbf{c}}_k$ are chosen so as to impose the convergence of $\mathbf{s}_{1,t}(t)$ and $\mathbf{s}_{2,t}(t)$ to the respective null steady state components within T_r according to (15). Consequently the convergence of $r_t(t)$ towards $\tilde{r}(t)$ is guaranteed. This assures the continuity of $r(t)$.

5. Robust estimation of $\mathbf{r}_t(t)$

This section shows how the MMCOP stated in Section 4 can be reformulated as a robust least square problem. The starting point is to rewrite the closed loop dynamical matrix $A_f(\alpha)$ as $A_f(\alpha) \triangleq \bar{A}_f + \delta A_f(\alpha)$, $\alpha \in \Lambda_l$ where \bar{A}_f is the nominal plant. Using the matrix identity $e^{(A+E)t} = e^{At} + \int_0^t e^{A(t-s)} E e^{A_s} ds$ and replacing A and E with \bar{A}_f and $\delta A_f(\alpha)$ respectively, one has

$$e^{(\bar{A}_f + \delta A_f(\alpha))t} = e^{\bar{A}_f t} + \int_0^t e^{\bar{A}_f(t-s)} \delta A_f(\alpha) e^{A_f(\alpha)s} ds \quad (24)$$

Then for any fixed $k = 0, 1, \dots, n_r - 1$, exploiting (24), the predicted $e(t_{k+i}|t_k)$ given by (21), can be rewritten as

$$\begin{aligned} e(t_{k+i}|t_k) &= y_d(t_{k+i}) - C_f e^{\bar{A}_f(t_{k+i}-t_k)} \hat{x}_f(t_k) \\ &- C_f \left[\int_0^{t_{k+i}-t_k} e^{\bar{A}_f(t_{k+i}-t_k-s)} \delta A_f(\alpha) e^{A_f(\alpha)s} ds \right] \hat{x}_f(t_k) \\ &- \int_{t_k}^{t_{k+i}} C_f e^{\bar{A}_f(t_{k+i}-\tau)} B_f \tilde{\mathbf{B}}(\tau) d\tau \tilde{\mathbf{c}}_k \\ &- \int_{t_k}^{t_{k+i}} C_f \left[\int_0^{t_{k+i}-\tau} e^{\bar{A}_f(t_{k+i}-\tau-s)} \delta A_f(\alpha) e^{A_f(\alpha)s} ds \right] B_f \tilde{\mathbf{B}}(\tau) d\tau \tilde{\mathbf{c}}_k \\ &- \int_{t_k}^{t_{k+i}} C_f e^{\bar{A}_f(t_{k+i}-\tau)} B_f \mathbf{y}_d(\tau) d\tau \\ &- \int_{t_k}^{t_{k+i}} C_f \left[\int_0^{t_{k+i}-\tau} e^{\bar{A}_f(t_{k+i}-\tau-s)} \delta A_f(\alpha) e^{A_f(\alpha)s} ds \right] B_f \mathbf{y}_d(\tau) d\tau \end{aligned}$$

or, equivalently,

$$e(t_{k+i}|t_k) = (b(t_{k+i}|t_k) + \delta b(t_{k+i}|t_k)) - (D(t_{k+i}|t_k) + \delta D(t_{k+i}|t_k)) f_k \quad (25)$$

where

$$\begin{aligned} b(t_{k+i}|t_k) &= y_d(t_{k+i}) - C_f e^{\bar{A}_f(t_{k+i}-t_k)} \hat{x}_f(t_k) \\ &- \int_{t_k}^{t_{k+i}} C_f e^{\bar{A}_f(t_{k+i}-\tau)} B_f \mathbf{y}_d(\tau) d\tau \end{aligned} \quad (26)$$

$$D(t_{k+i}|t_k) = \int_{t_k}^{t_{k+i}} C_f e^{\bar{A}_f(t_{k+i}-\tau)} B_f \tilde{\mathbf{B}}(\tau) d\tau \quad (27)$$

$$\begin{aligned} \delta b(t_{k+i}|t_k) &= -C_f \left[\int_0^{t_{k+i}-t_k} e^{\bar{A}_f(t_{k+i}-t_k-s)} \delta A_f(\alpha) e^{A_f(\alpha)s} ds \right] \hat{x}_f(t_k) \\ &\quad - \int_{t_k}^{t_{k+i}} C_f \left[\int_0^{t_{k+i}-\tau} e^{\bar{A}_f(t_{k+i}-\tau-s)} \delta A_f(\alpha) e^{A_f(\alpha)s} ds \right] B_f \mathbf{y}_d(\tau) d\tau \end{aligned} \quad (28)$$

$$\delta D(t_{k+i}|t_k) = \int_{t_k}^{t_{k+i}} C_f \left[\int_0^{t_{k+i}-\tau} e^{\bar{A}_f(t_{k+i}-\tau-s)} \delta A_f(\alpha) e^{A_f(\alpha)s} ds \right] B_f \tilde{\mathbf{B}}(\tau) d\tau \quad (29)$$

$$f_k = \tilde{\mathbf{c}}_k \quad (30)$$

Define the following vectors and matrices

$$\begin{aligned} \underline{e}_k &\triangleq [e^T(t_{k+1}|t_k), \dots, e^T(t_{k+(w-1)}|t_k)]^T \\ \underline{b}_k &\triangleq [b^T(t_{k+1}|t_k), \dots, b^T(t_{k+(w-1)}|t_k)]^T \\ \delta \underline{b}_k &\triangleq [\delta b^T(t_{k+1}|t_k), \dots, \delta b^T(t_{k+(w-1)}|t_k)]^T \end{aligned} \quad (31)$$

$$\begin{aligned} \underline{D}_k &\triangleq [D^T(t_{k+1}|t_k), \dots, D^T(t_{k+(w-1)}|t_k)]^T \\ \delta \underline{D}_k &\triangleq [\delta D^T(t_{k+1}|t_k), \dots, \delta D^T(t_{k+(w-1)}|t_k)]^T \\ \underline{Q}_k &\triangleq \text{diag}[Q(t_k), \dots, Q(t_k)], \end{aligned} \quad (32)$$

from the above definitions, it is evident that only $\delta \underline{b}_k$ and $\delta \underline{D}_k$ are depending on α . This dependence is now explicitly reintroduced to better clarify the formulation of the MMCOP as a robust least square problem.

Exploiting the above defined vectors and matrices, equations (26)-(30) can be expressed in the compact form

$$\underline{e}_k(\alpha) = (\underline{b}_k + \delta \underline{b}_k(\alpha)) - (\underline{D}_k + \delta \underline{D}_k(\alpha)) f_k,$$

and, for each $k = 0, \dots, n_r - 1$, functional $J_{k,\alpha}$ in (22) can be written as $J_{k,\alpha} = \underline{e}'_k(\alpha)^T \underline{e}'_k(\alpha)$, where $\underline{e}'_k(\alpha) \triangleq \underline{Q}_k^{1/2} \underline{e}_k(\alpha)$. Also defining $\underline{b}'_k + \delta \underline{b}'_k(\alpha) \triangleq \underline{Q}_k^{1/2} (\underline{b}_k + \delta \underline{b}_k(\alpha))$ and $\underline{D}'_k + \delta \underline{D}'_k(\alpha) \triangleq \underline{Q}_k^{1/2} (\underline{D}_k + \delta \underline{D}_k(\alpha))$, it is evident that each MMCOP is equivalent to the constrained minimization of the squared 2-norm of the worst-case weighted residual $\underline{e}'_k(\alpha)$. Hence the sequence of the n_r MMCOP (22), (23) is equivalent to solve the following sequence of Constrained Robust Least Square Problems (CRLSP).

$$\begin{aligned} \min_{f_k} \quad & \max_{\|\delta \underline{D}'_k(\alpha)\|_s \leq \rho_k, \|\delta \underline{b}'_k(\alpha)\|_s \leq \xi_k} \\ & \|(\underline{D}'_k + \delta \underline{D}'_k(\alpha)) f_k - (\underline{b}'_k + \delta \underline{b}'_k(\alpha))\|, \end{aligned} \quad (33)$$

$$\text{subject to } f_{k,\min} \leq f_k \leq f_{k,\max}, k = 0, 1, \dots, n_r - 1 \quad (34)$$

where: (33) is of the kind (4) and (34) is of the kind (6).

Theorem . Under Assumptions **A₁** and **A₂**, the feedforward input $r(t)$ of Σ_f resulting from the solution of the CRLSP (33), (34), and from the above RHC strategy, solves the RAEOTP.

Proof of Theorem

Transient condition: i) the convergence of $r_t(t)$ to $r_t(t_r^-) = \tilde{r}(t_r)$ follows from (16) taking into account the convex hull property of B-splines and the convergence to zero of the control points $\tilde{\mathbf{c}}_k$ over T_r ; ii) the transient $r_t(t)$ is the result of an RHC strategy applied to the minimization of the sequence of n_r "worst case" quadratic cost functionals (17). This requires the solution of the n_r MM-COP (22), (23), that is equivalent to solve the n_r CRLSP (33), (34).

Steady-state condition As Σ_f is robustly asymptotically stable and the controller contains an internal model of $\tilde{y}_d(t)$, then assumption **A₂** guarantees exact asymptotic tracking.

Boundedness condition For any uniformly bounded $y_d(t)$, the uniform boundedness of $r(t)$ follows from (16) and from the uniform boundedness of the two B-splines $\mathbf{s}_i(t)$, $i = 1, 2$. \triangle

Remark 3 Equations (11)-(13) define the state space representation of a linear dynamic feedback system forced by $r(t)$ and whose output is the dynamic output feedback signal $u(t)$. By (20) and (30), $r(t)$ is affinely depending on the new decision variables vector $f_k = \tilde{\mathbf{c}}_k$, with respect to which the cost functional $J_{k,\alpha}$ is minimized. Hence the MMCOP is here solved using a feedback prediction. This is useful to reduce the conservativeness of open loop Min-Max approach without using computationally demanding techniques (see e.g [38] -[41]). \triangle

5.1. A numerically simplified procedure for the solution of the CRLSP (33) (34)

According to Section 2.2, the sequence of CRLSP (33)-(34) can be formulated as

$$\min_{f_k} \|\underline{D}'_k f_k - \underline{b}'_k\| + \rho_k \|f_k\| + \xi_k \quad (35)$$

$$\text{subject to } f_{k,\min} \leq f_k \leq f_{k,\max}, k = 0, 1, \dots, n_r - 1 \quad (36)$$

By (35), (36), the numerical calculation of ρ_k and ξ_k can be greatly simplified taking into account the following:

- 1 As the term ξ_k of (35) is independent of f_k , it cannot be minimized. Hence it can be removed from the objective function. This implies that in (35) only the upper bound ρ_k on $\|\delta \underline{D}'_k(\alpha)\|_s$ needs to be determined at each k . Moreover, removing ξ_k also avoids computing the term $\delta \underline{b}'_k(\alpha) = \underline{Q}_k^{1/2} \delta \underline{b}_k(\alpha)$. The calculation of this term would require the numerically involved computation of the r.h.s. of (28) for $i = 1, \dots, w - 1$. As the term (28) depends on $\hat{x}_f(t_k)$, its calculation would necessarily involve an onerous on line computational burden.
- 2 The way the B-spline basis functions are defined by the Cox de Boor formula [34], implies that $\tilde{\mathbf{B}}(\tau) = \tilde{\mathbf{B}}(\tau + t_w)$, $\forall \tau \in [t_k, t_k + t_w)$, $k =$

$0, 1, \dots, n_r - 1$. Hence, by (29) and (32) and recalling that $\delta \underline{D}'_k(\alpha) = Q_k^{1/2} \delta \underline{D}_k(\alpha)$ one has that $\rho_k \triangleq \rho, \forall k = 0, 1, \dots, n_r - 1$.

- 3 By point 2, the calculation of ρ can be entirely executed off-line performing a gridding on the parameter vector $\alpha \in \Lambda_I$.

6. Numerical results

The robust trajectory tracking problem considered in this section is a more involved version of the stabilization problem considered in [35]. The linearized model (37) is the unstable, non minimum phase with near non hyperbolic internal dynamics system considered in [35]. It represents an aircraft trimmed at a nominal 5° pitch attitude, with a mid-range weight, a mid-position center of gravity and operating in-ground effect at near sea level. The model is described by

$$\dot{x}_p(t) = A_p x_p(t) + B_p u(t), \quad y(t) = C_p x_p(t) \quad (37)$$

where

$$\begin{aligned} x_p &= \begin{pmatrix} U \\ W \\ Q \\ V \\ P \\ R \\ \theta \\ \chi \end{pmatrix} = \begin{pmatrix} \text{forward velocity} \\ \text{vertical velocity} \\ \text{pitch rate} \\ \text{lateral velocity} \\ \text{roll rate} \\ \text{yaw rate} \\ \text{pitch attitude} \\ \text{roll attitude} \end{pmatrix}, \quad y = \begin{pmatrix} U \\ W \\ V \\ R \end{pmatrix} \\ u &= \begin{pmatrix} \delta_C \\ \delta_B \\ \delta_A \\ \delta_P \end{pmatrix} = \begin{pmatrix} \text{collective} \\ \text{longitudinal cyclic} \\ \text{lateral cyclic} \\ \text{tail rotor collective} \end{pmatrix} \end{aligned}$$

The vectors $y(t) \in \mathbb{R}^q$, $u(t) \in \mathbb{R}^m$, $q = m = 4$, represent the controlled and manipulated variables respectively. Like [35], the state vector $x_p(t) \in \mathbb{R}^n$, $n = 8$, is assumed to be measurable. The entries of A_p and of B_p (not reported for brevity) can be found in [35], matrix C_p directly follows by the way $y(t)$ is defined.

With respect to [35], a polytopic dynamical matrix $A_p(\alpha)$ is here assumed. The dynamical matrix A_p reported in [35] is considered the nominal matrix \bar{A}_p of $A_p(\alpha)$.

The three elements $a_{i,i}$, $i = 2, 3, 5$ of $A_p(\alpha)$, have been here assumed to belong to the intervals $[\bar{a}_i - \varepsilon_{a_{i,i}}, \bar{a}_i + \varepsilon_{a_{i,i}}]$, $i = 2, 3, 5$, centered on the nominal value \bar{a}_i where: $\bar{a}_2 = -0.39$, $\bar{a}_3 = -0.19$ and $\bar{a}_5 = -0.57$. Three possible uncertainty scenarios are considered $\mathcal{S}_1 = (\varepsilon_{a_{2,2}}^{(1)}, \varepsilon_{a_{3,3}}^{(1)}, \varepsilon_{a_{5,5}}^{(1)}) = (0.39, 0.19, 0.57)$, $\mathcal{S}_2 = (\varepsilon_{a_{2,2}}^{(2)}, \varepsilon_{a_{3,3}}^{(2)}, \varepsilon_{a_{5,5}}^{(2)}) = (0.29, 0.09, 0.43)$, $\mathcal{S}_3 = (\varepsilon_{a_{2,2}}^{(3)}, \varepsilon_{a_{3,3}}^{(3)}, \varepsilon_{a_{5,5}}^{(3)}) = (0.15, 0.05, 0.22)$.

For any \mathcal{S}_v , $v = 1, 2, 3$, the respective uncertain open loop plant $A_p(\alpha)$ belongs to the polytopic set $\mathcal{A} \triangleq \{A_p(\alpha) = \sum_{i=1}^l \alpha_i A_{p_i}, \alpha \in \Lambda_l\}$ with $l = 8$.

As in [35], the forward velocity and the yaw rate are to be kept at zero $\forall t \in \mathbb{R}^+$, while the desired behavior of W and V is the smooth function converging to the constant value 0.2 in the interval $T_y = [0, t_y] = [0, 13]$, as shown in Figure 2. Unlike [35], the unnecessity of a pre-actuation in the proposed approach allowed us to freely assign the desired profiles without requiring them to be null over an initial sufficiently long time interval.

The first step is the design of a robustly stabilizing feedback controller. As the state is assumed to be measurable, the observer Σ_o is not necessary. This directly implies that the control input $u(t)$ is given by $u(t) = -K_p x_p(t) + K_c x_c(t) + r_2(t)$. The gain matrices K_p and K_c defining a robustly stabilizing controller for \mathcal{S}_1 (a fortiori for $\mathcal{S}_2, \mathcal{S}_3$) have been computed imposing the following eigenvalues $[-0.7 \pm 0.73i, -2 \pm 1.5i, -5, -5.5, -4.95, -3, -2.8, -2.24, -0.61, -0.33]$ to the nominal closed loop dynamical matrix $\bar{A}_f = \begin{bmatrix} \bar{A}_p & 0 \\ -B_c C_p & A_c \end{bmatrix} - \begin{bmatrix} B_p \\ 0 \end{bmatrix} [K_p \quad -K_c]$.

For the given $\Sigma_p \equiv (C_p, A_p(\alpha), B_p)$, it is easy to verify that the system matrix $\begin{bmatrix} sI - A_p(\alpha) & B_p \\ -C_p & 0 \end{bmatrix}$ has rank $n + q = 12$ at $s = 0, \forall \alpha \in \Lambda_l$. This implies the fulfillment of **A2** and, as a consequence, guarantees an exact steady-state tracking, provided endowing the stabilizing controller with the internal model Σ_c of the external reference [37]. As $\tilde{y}_d(t) \in \mathbb{R}^q$, $q = 4$, then the internal model Σ_c of constant signals is defined by $A_c = 0_{q \times q} = 0_{4 \times 4}$ and $B_c = I_{q \times q} = I_{4 \times 4}$.

The second step is to compute the input $r(t)$ solving the **RAEOT** problem. According to Section 4.1 one has $\tilde{r}(t) = [\tilde{y}_d^T(t) \quad \mathbf{0}_m^T]^T, \forall t \geq t_r$ where: $\mathbf{0}_\ell$ denotes the column vector of ℓ null elements and $t_r = t_s = 25$ is chosen. Both the transient components $s_{1,t}(t) \in \mathbb{R}^q$, and $s_{2,t}(t) \in \mathbb{R}^m$, defining $r_t(t) \triangleq \begin{bmatrix} y_d(t) + \mu_1 s_{1,t}(t) \\ \mu_2 s_{2,t}(t) \end{bmatrix}$ have been modeled as two B spline functions vectors with $d_1 = d_2 = 1$ (order of the B-spline function) and $\ell_1 = \ell_2 = 4$ (number of control points defining the B-spline function over each moving window of length t_w). Fig. 2 evidences a desired $y_{d,t}(t)$, $t \in T_y$, given by two fast but smooth transitions between two set points. The time interval of each transition is $t_{tr} = 2$ and the value $t_w = t_{tr} = 2$ is chosen. By (20) it directly follows that $\tilde{\mathbf{c}} \triangleq \begin{bmatrix} \bar{\mathbf{c}}_1 \\ \bar{\mathbf{c}}_2 \end{bmatrix} \in \mathbb{R}^{q\ell_1 + m\ell_2 = 32}$, $\bar{\mathbf{B}}_{d_1}(t)$ has dimensions $q \times q\ell_1$ and $\bar{\mathbf{B}}_{d_2}(t)$ has dimensions $m \times m\ell_2$.

As $t_r = 30$ and $t_w = 2$ one has $T'_r = [0, 32]$ and choosing $n_r = 300$ one has $\Delta = 0.1$ and $w = 20$.

The vector $f_k \triangleq \tilde{\mathbf{c}}_k$ defining $r_t(t)$ over each moving prediction horizon $[t_k, t_k + t_w) = [t_k, t_{k+w})$, $k = 0, \dots, n_r - 1 = 299$, is iteratively estimated solving the sequence of n_r CRLSP (33),(34), using the software Yalmip [42]. All the weight matrices $Q(t_k)$ are set equal to the identity matrix. A large interval $[f_{k,\min}, f_{k,\max}]$ is initially chosen to allow $r_t(t)$ to freely vary at the be-

ginning of the transition period $0 \leq k \leq k_y \triangleq \frac{t_y}{\Delta}$. For $k > k_y$, $f_{k,\min}$ and $f_{k,\max}$ (namely $s_{1,t}(t)$ and $s_{2,t}(t)$) converge to zero in such a way that $r_t(t) \rightarrow \tilde{r}(t_r)$ for $t \rightarrow t_r$. A general rule to fix the vectors $f_{k,\max}$, and $f_{k,\min}$, $k = 0, 1, \dots, n_r - 1$, is: $f_{k,\max} = |f_{k,\min}| = \begin{cases} f \mathcal{I}_1 & 0 \leq k \leq k_y \\ f e^{-\beta(k-k_y)} \mathcal{I}_1 & k_y \leq k \leq n_r - 1 \end{cases}$ where \mathcal{I}_1 denotes a column vector of $(q\ell_1 + m\ell_2)$ elements equal to 1. In this case $f = 5$, $\beta = 0.4$ and $k_y = 130$ are set.

With reference to each \mathcal{S}_i , $i = 1, 2, 3$, three simulations relative to FFCLI, FFPI and FFOBI control schemes have been performed starting from null initial conditions and choosing: $\alpha \in \Lambda_8$ with $\alpha_5 = 1$ and $\alpha_l = 0$, $l \neq 5$.

Tables 1-3 report the 2-norm of the tracking error $e(t) \triangleq y_d(t) - y(t)$, the 2-norms of $\mathbf{s}_{1,t}(t)$ and $\mathbf{s}_{2,t}(t)$ over $T_r = [0, 30)$ and the value of ρ relative to each scenario \mathcal{S}_i , $i=1,2,3$. The same tables show that in all the three considered scenarios the FFOBI control scheme outperforms both FFCLI and FFPI because it provides the minimum 2-norm of the transient tracking error. This is produced by an optimal combination of FFCLI and FFPI, whose weights are given by the 2-norm of the B-splines $s_{1,t}(t)$ and $s_{2,t}(t)$ respectively.

It is also noticed that FFCLI gives better tracking performance with respect to FFPI. This is in accordance with the simulations reported in [23], [26].

A measure of the improvement provided by the FFOBI has been calculated as the percentage of reduction of $\|e\|_2$ with respect to FFCLI and FFPI. These percentages, denoted by $P_{OBI/CLI}$ and $P_{OBI/PI}$, are reported in Table 4. Figures 2, 3 and 4 (relative to \mathcal{S}_1 , \mathcal{S}_2 and \mathcal{S}_3 respectively) show the behavior of the controlled output $y(t) \triangleq [U(t) \ W(t) \ V(t) \ R(t)]^T$ produced by the FFOBI, FFCLI and FFPI schemes respectively.

Table 1: Scenario 1: The 2-norm of the tracking error $e(t)$ and the 2-norms of $\mathbf{s}_{1,t}(t)$ and $\mathbf{s}_{2,t}(t)$, over $T_r = [0, 30)$.

$(\varepsilon_{a_{2,2}}^{(1)}, \varepsilon_{a_{3,3}}^{(1)}, \varepsilon_{a_{5,5}}^{(1)}) = (0.39, 0.19, 0.57), \rho = 0.1002$			
	$\ e(t)\ _2$	$\ \mathbf{s}_{1,t}(t)\ _2$	$\ \mathbf{s}_{2,t}(t)\ _2$
FFOBI	0.8204	12.7564	5.5891
FFCLI	1.0376	14.0837	0
FFPI	4.7380	0	29.2785

Table 2: Scenario 2: The 2-norm of the tracking error $e(t)$ and the 2-norms of $\mathbf{s}_{1,t}(t)$ and $\mathbf{s}_{2,t}(t)$, over $T_r = [0, 30)$.

$(\varepsilon_{a_{2,2}}^{(2)}, \varepsilon_{a_{3,3}}^{(2)}, \varepsilon_{a_{5,5}}^{(2)}) = (0.29, 0.09, 0.43), \rho = 0.0685$			
	$\ e(t)\ _2$	$\ \mathbf{s}_{1,t}(t)\ _2$	$\ \mathbf{s}_{2,t}(t)\ _2$
FFOBI	0.6758	13.9686	7.2225
FFCLI	0.7950	16.2166	0
FFPI	3.6100	0	60.0232

Table 3: Scenario 3: The 2-norm of the tracking error $e(t)$ and the 2-norms of $\mathbf{s}_{1,t}(t)$ and $\mathbf{s}_{2,t}(t)$, over $T_r = [0, 30)$.

$(\varepsilon_{a_{2,2}}^{(3)}, \varepsilon_{a_{3,3}}^{(3)}, \varepsilon_{a_{5,5}}^{(3)}) = (0.15, 0.05, 0.22), \rho = 0.0221$			
	$\ e(t)\ _2$	$\ \mathbf{s}_{1,t}(t)\ _2$	$\ \mathbf{s}_{2,t}(t)\ _2$
FFOBI	0.3434	12.4889	6.5979
FFCLI	0.3861	13.1025	0
FFPI	3.6731	0	57.0717

Table 4: The percentage of reduction of $\|e\|_2$ provided by FFOBI with respect to FFCLI and FFPI in the three scenarios.

	$P_{OBI/CLI}$	$P_{OBI/PI}$
Scenario 1	20.93 %	82.68%
Scenario 2	14.99 %	81.28%
Scenario 3	11.05 %	90.65%

7. Conclusions

In the context of approximated model inversion based control, a new and more general 2DoF control architecture has been proposed here. It consists of an optimally weighted combination of FFPI and FFCLI control schemes. The numerical results confirmed that the best tracking performance is given by the FFOBI configuration.

The three main appealing features of the proposed approach can be summarized as: 1) generality of application, 2) robustness with respect to parametric uncertainties, 3) a numerically simplified procedure for the solution of min-max optimization problems (33), (34). The first one makes the method amenable to be applied in a large and diversified class of control problems. The second one provides an answer to the long standing problem concerning the application of inversion based feedforward control in the case of uncertain plants. The third greatly reduces the numerical complexity of the overall RHC strategy.

References

- [1] S. Devasia, D. Chen, B. Paden, "Nonlinear inversion based output tracking", *IEEE Transactions on Automatic Control*, Vol. 41, 1996, pp. 930-942.
- [2] L. R. Hunt, G. Meyer, R. Su, "Non-causal inverses for linear systems", *IEEE Transactions on Automatic Control*, Vol. 41, 1996, pp. 608-611.
- [3] Q. Zou, S. Devasia, "Preview based stable inversion for output tracking of linear systems", *Journal of Dynamic Systems Measurement and Control*, Vol. 121, pp. 625-630, 1999.

- [4] Q. Zou, "Optimal preview-based stable-inversion for output tracking of nonminimum-phase linear systems", *Automatica*, Vol. 45, 2009, pp. 230-237.
- [5] H. Perez, S. Devasia, "Optimal output-transition for linear systems", *Automatica*, Vol. 39, pp.181-192, 2003.
- [6] L. Jetto, V. Orsini, R. Romagnoli, " A mixed numerical-analytical stable pseudo-inversion method aimed at attaining an almost exact tracking", *Intern. Journal of Robust and Nonlinear Control*, Vol. 25, pp. 809-823, 2015.
- [7] E. Naderi, K. Khorasani, "Inversion-based output tracking and unknown input reconstruction of a square discrete-time linear system", *Automatica*, Vol.95, pp. 44-53, 2018.
- [8] J. V. Zundert, T. Oomen, "On inversion- based approaches for feedforward and ILC", *Mechatronics*, Vol. 50, pp. 282-291, 2018.
- [9] A. Costalunga, A. Piazzzi, "A behavioural approach to inversion-based control", *Automatica*, Vol. 95, pp. 433-455, 2018.
- [10] R. Romagnoli, E. Garone, "A general framework for approximated model stable inversion", *Automatica*, Vol. 101, pp. 182-189, 2019.
- [11] A. Minari, A. Piazzzi, A. Costalunga, "Polynomial interpolation for inversion-based control", *European Journal of Control*, Vol. 56, pp. 62-72, 2020.
- [12] S. Devasia, "Should model-based inverse inputs be used as feedforward under plant uncertainty?", *IEEE Transactions on Automatic Control*, Vol. 47, pp. 1865-1871, 2002.
- [13] K. K.Leang , S. Devasia, "Feedback-linearized inverse feedforward for creep hysteresn and vibration compensation in AFM piezoactuators", *IEEE Control Systems Technology*, Vol. 15, pp. 927-935, 2007.
- [14] Y. Wu, Q. Zou, "Robust inversion-based 2-DOF control design for output tracking: piezoelectric-actuator example", *IEEE Control Systems Technology*, Vol. 17, pp.1069-1082, 2009.
- [15] C. Peng, H. Xu, Q. Zou, J. Zhang, "Inversion-based robust feedforward-feedback two-degree-of-freedom control approach for multi-input multi-output system with uncertainty", *IET Control Theory and Applications*, Vol. 6, pp. 2279-2291, 2011.
- [16] Y. Xie, A. Alleyne, "Robust Two Degree-Of-Freedom Control for MIMO System with Both Model and Signal Uncertainties", *Proceedings of the 19th IFAC World Congress*, Cape Town, South Africa, pp. 9313-9320, 2014.

- [17] C.Peng, C. Han, J.Zou, G. Zhang, " H_∞ Optimal inversion feedforward and robust feedback based 2DOF control approach for high speed precision positioning systems", *Journ. of Control Science and Engineering*, Vol. 2, pp. 1-11, 2016.
- [18] R. Jeyasenthil, S.B. Choi, H. Purohit, D. Jung, "Robust position and disturbance rejection of an industrial plant emulator system using the feedforward-feedback control", *Mechatronics*, Vol. 57, pp. 29-38, 2019.
- [19] A.Piazzi, A. Visioli, "Optimal inversion-based control for the set-point regulation of nonminimum-phase uncertain scalar systems", *IEEE Transactions on Automatic Control*, Vol.46, pp. 1654-1659, 2001.
- [20] A. Piazzi, A. Visioli, "Optimal dynamic inversion-based control of an overhead crane, IEE Proc. Control Theory Appl., Vol. 149, pp. 405-411, 2002.
- [21] K.Leang, S. Devasia," Feedback linearized inverse feedforward for creep hysteresis, and vibration compensation in AFM piezoactuators", *IEEE Trans. Control System Technology*, Vol. 15, pp. 927-935, 2007.
- [22] S. S. Aphale, S. Devasia, S.O.R. Moheimani, "High-bandwidth control of a piezoelectric nanopositioning stage in the presence of plant uncertainties", *Nanotechnology*, Vol. 19, pp. 125503-125511, 2008.
- [23] B.P. Rigney, L.Y. Pao, D.A Lawrence, "Model inversion architectures for settle time applications with uncertainty", *45th IEEE Control Decis. Conf.*, San Diego (CA), 2006.
- [24] S. Devasia, E. Eleftheriou, R. Moheimani, "A survey of control issues in nanopositioning", *IEEE Trans. Control System Technology*, Vol.15, pp.802-823, 2007.
- [25] J.A. Butterworth, L.Y. Pao, D.Y. Abramovitch, "Architectures for tracking control in atomic force microscopes", *17th IFAC World Congress*, Seoul, Korea, 2006.
- [26] J.A. Butterworth, L.Y. Pao, D.Y. Abramovitch, "A comparison of control architectures for atomic force microscopes", *Asian Journal of Control*, Vol. 11, pp.175-181, 2009.
- [27] G.M. Clayton, S. Tien, K.K. Leang, Q. Zou, S. Devasia, "A review of feed-forward control approaches in nanopositioning for high-speed SPM", *Journal of Dynamic Systems, Measurement, and Control*, Vol.131, pp. 061101-1 061101-19, 2009.
- [28] J . Kavaja, A. Piazzi, "On the equivalence of model inversion architectures for control applications," *2020 59th IEEE Conference on Decision and Control*, Jeju Island, Republic of Korea, 2020.

- [29] L. Jetto, V. Orsini, R. Romagnoli, "Optimal transient performance under output set-point reset", *Intern. Journal of Robust and Nonlinear Control*, Vol. 26, pp. 2788-2805, 2016.
- [30] L. Jetto and V. Orsini, "Robust pseudo-inversion of polytopic systems using second order cone programming", *28th IEEE Mediterranean Conference on Control and Automation*, Saint-Raphael, France, 2020.
- [31] L. Jetto, V. Orsini and R. Romagnoli, "Two degrees of freedom control and B-spline functions as tools for a reduced complexity approach to MPC", *American Control Conference*, Denver, Colorado, 2020.
- [32] L. Jetto, V. Orsini, "A robust least squares based approach to min-max model predictive control", *Intern. Journal of Robust and Nonlinear Control*, Vol 30, pp. 4807- 4825, 2020.
- [33] L. Jetto, V. Orsini, "An optimally combined feedback/feedforward control architecture for minimizing the oscillations in the fast response of a gantry crane control system" *29th Mediterranean Conference on Control and Automation*, Bari, Italy, 2021.
- [34] C. De Boor (1978). "A practical guide to splines", Springer Verlag, New York.
- [35] S. Devasia, "Output Tracking with Nonhyperbolic and Near Nonhyperbolic Internal Dynamics: Helicopter Hover Control", *J. of Guidance, Control and Dynamics*, Vol 20, pp. 573-580, 1997.
- [36] M.S. Lobo, L. Vandenberghe, S. Boyd, H. L  bret, "Applications of second-order cone programming", *Linear Algebra and its Applications*, Vol. 284, pp. 193-228, 1998.
- [37] C.A. Desoer, Y.T. Wang, "Linear time invariant robust servomechanism problem: a self contained exposition", *Control and Dynamic Systems* C.T. Leondes (Ed.), Vol. 16, pp. 81-129,1980.
- [38] L. Chisci, P. Falugi, G. Zappa, "Predictive control for constrained systems with polytopic uncertainty", *American Control Conference*, Arlington, VA, USA, 2001.
- [39] A. Bemporad, F. Borrelli, M.Morari, "Min-Max control of constrained uncertain discrete-time linear systems", *IEEE Transactions on Automatic Control*, Vol.48, pp. 1600-1606, 2003.
- [40] Fukushima, Bitmead, "Robust constrained model predictive control using closed-loop prediction", *American Control Conference*, Denver, Colorado, 2003.
- [41] J. Lofberg, "Approximations of closed-loop minimax MPC", *42nd IEEE Control Decision Conference*, Hawaii, USA, 2003.

- [42] J. Löfberg, <https://yalmip.github.io>
- [43] Y. Zhao, Jayasuriya, "Feedforward controllers and tracking accuracy in the presence of plant uncertainties", *ASME J. Dynamic Systems Measurement and Control*, Vol.117, pp. 490-495, 1995.
- [44] S. Boyd, L. El Ghaoui, E. Feron and V. Balakrishnan. Linear Matrix Inequalities in System and Control Theory 1994;15 of Studies in Applied Mathematics Society for Industrial and Applied Mathematics (SIAM).

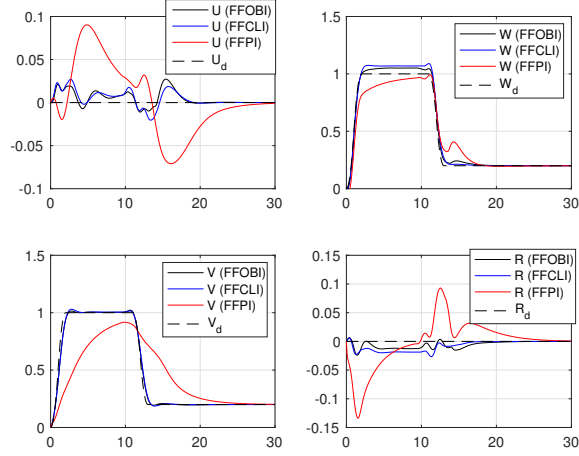


Figure 2: Scenario 1: The trajectories of $y_d(t) \triangleq [U_d(t) \ W_d(t) \ V_d(t) \ R_d(t)]^T$ (black dashed lines) and of the controlled output $y(t) \triangleq [U(t) \ W(t) \ V(t) \ R(t)]^T$ produced by FFOBI (black lines), FFCLI (blue lines) and FFPI (red lines) schemes respectively.

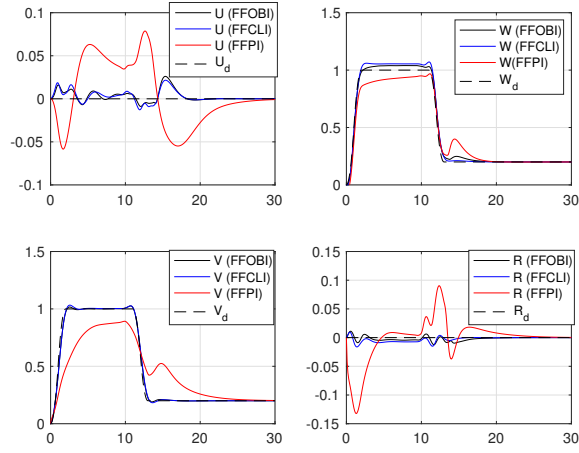


Figure 3: Scenario 2: The trajectories of $y_d(t) \triangleq [U_d(t) \ W_d(t) \ V_d(t) \ R_d(t)]^T$ (black dashed lines) and of the controlled output $y(t) \triangleq [U(t) \ W(t) \ V(t) \ R(t)]^T$ produced by FFOBI (black lines), FFCLI (blue lines) and FFPI (red lines) schemes respectively.

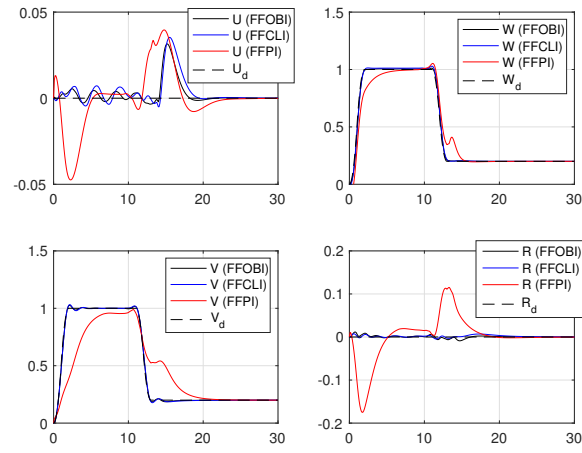


Figure 4: Scenario 3: The trajectories of $y_d(t) \triangleq [U_d(t) \ W_d(t) \ V_d(t) \ R_d(t)]^T$ (black dashed lines) and of the controlled output $y(t) \triangleq [U(t) \ W(t) \ V(t) \ R(t)]^T$ produced by FFOBI (black lines), FFCLI (blue lines) and FFPI (red lines) schemes respectively.